

Crystal Structures and Thermal Properties of L-MnC₄H₄O₆ · 2H₂O and DL-MnC₄H₄O₆ · 2H₂O

Takanori Fukami¹, Shuta Tahara¹

¹Department of Physics and Earth Sciences, Faculty of Science, University of the Ryukyus, Japan

Correspondence: Takanori Fukami, Department of Physics and Earth Sciences, Faculty of Science, University of the Ryukyus, Okinawa 903-0213, Japan. E-mail: fukami@sci.u-ryukyu.ac.jp

Received: November 21, 2019 Accepted: December 16, 2019 Online Published: December 30, 2019

doi:10.5539/ijc.v12n1p78

URL: <https://doi.org/10.5539/ijc.v12n1p78>

Abstract

Manganese L-tartrate dihydrate, L-MnC₄H₄O₆ · 2H₂O, and manganese DL-tartrate dihydrate, DL-MnC₄H₄O₆ · 2H₂O, crystals were grown at room temperature by the gel method using silica gels as the growth medium. Differential scanning calorimetry, thermogravimetric-differential thermal analysis, and X-ray diffraction measurements were performed on both crystals. The space group symmetries (monoclinic *P*₂₁ and *P*₂/*c*) and structural parameters of the crystals were determined at room temperature. Both structures consisted of slightly distorted MnO₆ octahedra, C₄H₄O₆ and H₂O molecules, and O–H··O hydrogen-bonding frameworks between adjacent molecules. Weight losses due to thermal decomposition of the crystals were found to occur in the temperature range of 300–1150 K. We inferred that the weight losses were caused by the evaporation of bound 2H₂O molecules, and the evolutions of gases from C₄H₄O₄ and of (1/2)O₂ gas from MnO₂, and that the residual black substance left in the vessels after decomposition was manganese oxide (MnO).

Keywords: L-MnC₄H₄O₆ · 2H₂O, DL-MnC₄H₄O₆ · 2H₂O, crystal structure, thermal decomposition, TG-DTA, X-ray diffraction

1. Introduction

Many tartrate compounds are formed by reacting tartaric acid with compounds containing positive ions (two monovalent cations or one divalent cation) (Desai & Patel, 1988; Fukami, Hiyajyo, Tahara, & Yasuda, 2017a; Fukami, Hiyajyo, Tahara, & Yasuda, 2017b; Fukami & Tahara, 2018; Labutina, Marychev, Portnov, Somov, & Chuprunov, 2011). Tartaric acid (chemical formula: C₄H₆O₆; systematic name: 2,3-dihydroxybutanedioic acid) has two chiral carbon atoms in its structure, which provides the possibility for four possible different forms of chiral, racemic, and achiral isomers: L(+)-tartaric, D(-)-tartaric, racemic (DL-) tartaric, and meso-tartaric acid (Bootsma & Schoone, 1967; Fukami, Tahara, Yasuda, & Nakasone, 2016; Song, Teng, Dong, Ma, & Sun, 2006). Some of these compounds are of interest because of their physical properties, particularly their excellent dielectric, ferroelectric, piezoelectric, and nonlinear optical properties (Abdel-Kader et al., 1991; Firdous, Quasim, Ahmad, & Kotru, 2010; Torres et al., 2002). Moreover, they were formerly used in numerous industrial applications, for example, as transducers and in linear and non-linear mechanical devices.

Experimental studies on manganese tartrate crystals (containing two or four water molecules) were conducted as follows (Labutina, Marychev, Portnov, Somov, & Chuprunov, 2011; Soylyu, 1985; Yanes, Lopez, Stockel, Peraza, & Torres, 1996). Soylyu has reported the crystal structure of MnC₄H₄O₆ · 4H₂O at room temperature determined by single-crystal X-ray diffraction (Soylyu, 1985). The structure was found to be monoclinic with space group *P*₂₁, the lattice constants being *a* = 6.092(5), *b* = 12.285(7), *c* = 7.295(4) Å and β = 112°, and consisted of strongly disordered MnO₆ octahedra and C₄H₄O₆ molecules. Each manganese atom was surrounded by six oxygen atoms, four from two chelate rings of two tartrate ions and two water molecules. Moreover, the atoms linked the tartrate molecules to infinite chains parallel to the [100] direction. Labutina et al. have grown many tartrate single crystals by the gel method, and determined the crystal system and lattice constants (Labutina, Marychev, Portnov, Somov, & Chuprunov, 2011). The crystal structure of MnC₄H₄O₆ · 2H₂O was reported to be monoclinic with space group *P*₂₁ and the lattice constants *a* = 7.60834(1), *b* = 11.1482(2), *c* = 8.9349(7) Å and β = 99.433(2). Yanes et al. have also grown manganese tartrate crystals by the gel method, and performed measurements of dielectric and magnetic properties, infrared spectroscopic, thermal studies, and X-ray diffraction on the crystals (Yanes, Lopez, Stockel, Peraza, & Torres, 1996). Their basic physical properties observed were reported. Moreover, thermogravimetric analysis suggested that the grown crystals were

associated with two molecules of water of hydration, and that the material was reduced to its oxide by thermal decomposition.

As mentioned above, it is expected that a manganese DL-tartrate compound can be synthesized using Mn^{2+} ions as the divalent cations and DL-tartaric acid. The crystal structure of $\text{MnC}_4\text{H}_4\text{O}_6 \cdot 2\text{H}_2\text{O}$ containing two water molecules has not been determined yet, except for its crystal system and lattice constants. In this paper, we describe the synthesis of manganese L-tartrate dihydrate $\text{L-MnC}_4\text{H}_4\text{O}_6 \cdot 2\text{H}_2\text{O}$ and manganese DL-tartrate dihydrate $\text{DL-MnC}_4\text{H}_4\text{O}_6 \cdot 2\text{H}_2\text{O}$ crystals by the gel method, and also determine their crystal structures at room temperature using single-crystal X-ray diffraction. Moreover, the thermal properties of these crystals are studied by means of differential scanning calorimetry (DSC) and thermogravimetric-differential thermal analysis (TG-DTA).

2. Experimental

2.1 Crystal Growth

The $\text{L-MnC}_4\text{H}_4\text{O}_6 \cdot 2\text{H}_2\text{O}$ and $\text{DL-MnC}_4\text{H}_4\text{O}_6 \cdot 2\text{H}_2\text{O}$ crystals were grown in silica gel medium at room temperature using the single test tube diffusion method. The gels for $\text{L-MnC}_4\text{H}_4\text{O}_6 \cdot 2\text{H}_2\text{O}$ were prepared in test tubes (length of 200 mm, and diameter of 30 mm) using aqueous solutions of Na_2SiO_3 (25 ml of 1 M), $\text{L-C}_4\text{H}_6\text{O}_6$ (25 ml of 1 M), and CH_3COOH (25 ml of 2 M). For $\text{DL-MnC}_4\text{H}_4\text{O}_6 \cdot 2\text{H}_2\text{O}$, the gels were prepared in test tubes using aqueous solutions of Na_2SiO_3 (20 ml of 1 M), $\text{DL-C}_4\text{H}_6\text{O}_6$ (25 ml of 1 M), and CH_3COOH (25 ml of 1 M). The gels were aged for nine days, and solutions of $\text{MnCl}_2 \cdot 4\text{H}_2\text{O}$ (25 ml of 0.5 M) were then gently poured on top of the respective gels. The crystals were harvested after about three months. Figure 1 shows the photographs of (a) $\text{L-MnC}_4\text{H}_4\text{O}_6 \cdot 2\text{H}_2\text{O}$ single crystals grown on the gel surface, and of slightly pinkish crystals of (b) $\text{L-MnC}_4\text{H}_4\text{O}_6 \cdot 2\text{H}_2\text{O}$ and (c) $\text{DL-MnC}_4\text{H}_4\text{O}_6 \cdot 2\text{H}_2\text{O}$ grown in the gel medium. Large single crystals of $\text{DL-MnC}_4\text{H}_4\text{O}_6 \cdot 2\text{H}_2\text{O}$ could not be grown in the gel medium or on the gel surface, under some growth medium gel concentrations including the concentration for $\text{L-MnC}_4\text{H}_4\text{O}_6 \cdot 2\text{H}_2\text{O}$ single crystals. The shape and color of the pinkish crystals obtained were very similar to that obtained by Yanes et al (Yanes, Lopez, Stockel, Peraza, & Torres, 1996).

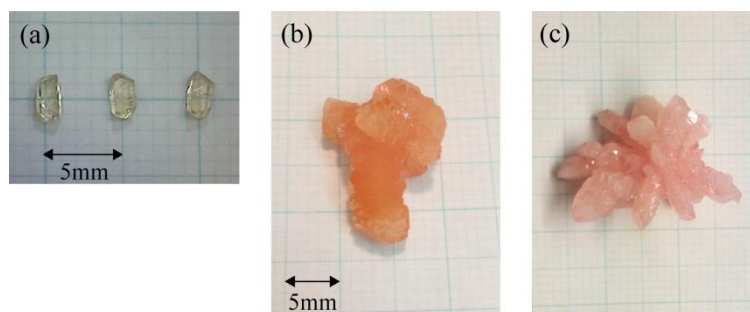


Figure 1. Photographs of (a) $\text{L-MnC}_4\text{H}_4\text{O}_6 \cdot 2\text{H}_2\text{O}$ single crystals grown on the gel surface, and of slightly pinkish crystals of (b) $\text{L-MnC}_4\text{H}_4\text{O}_6 \cdot 2\text{H}_2\text{O}$ and (c) $\text{DL-MnC}_4\text{H}_4\text{O}_6 \cdot 2\text{H}_2\text{O}$ grown in the gel medium

2.2 Structure Determination

The X-ray diffraction measurements were carried out using a Rigaku Saturn CCD X-ray diffractometer with graphite-monochromated $\text{Mo } K_\alpha$ radiation ($\lambda=0.71073 \text{ \AA}$). The diffraction data were collected at 299 K using an ω scan mode with a crystal-to-detector distance of 40 mm, and processed using the CrystalClear software package. The intensity data were corrected for Lorentz polarization and absorption effects. The structures were solved by direct methods using the SIR2011 program and refined on F^2 by full-matrix least-squares methods using the SHELXL-2013 program in the WinGX package (Burla et al., 2012; Farrugia, 2012; Sheldrick, 2015). Samples of $\text{L-MnC}_4\text{H}_4\text{O}_6 \cdot 2\text{H}_2\text{O}$ and $\text{DL-MnC}_4\text{H}_4\text{O}_6 \cdot 2\text{H}_2\text{O}$ used in the X-ray measurements were cut from the single crystal and from a very small transparent crystal grown on the pinkish crystal surface, respectively.

2.3 Thermal Measurements

DSC and TG-DTA measurements were carried out in the temperature ranges of 100–310 K and 300–1470 K, respectively, using DSC7020 and TG-DTA7300 systems from Seiko Instruments Inc. Aluminium (for DSC) and platinum (for TG-DTA) open pans were used as measuring vessels and reference pans. Fine powder samples of $\text{L-MnC}_4\text{H}_4\text{O}_6 \cdot 2\text{H}_2\text{O}$ and $\text{DL-MnC}_4\text{H}_4\text{O}_6 \cdot 2\text{H}_2\text{O}$ for the thermal measurements were prepared by grinding some pieces from the single crystal and some transparent ones at the tip of the pinkish crystal, respectively. The sample amount varied between 3.92 and 5.20 mg, and the heating rates were 10 K min^{-1} under a flow of nitrogen gas (40 ml min^{-1} for DSC, and 300 ml min^{-1} for TG-DTA).

3. Results and Discussion

3.1 Crystal Structure

The crystal structures of L-MnC₄H₄O₆·2H₂O and DL-MnC₄H₄O₆·2H₂O were determined at room temperature using the single-crystal X-ray diffraction method. The lattice parameters calculated from all the observed X-ray reflections showed that both crystals belong to a monoclinic system. The systematic extinctions of the reflections from L-MnC₄H₄O₆·2H₂O revealed that the space group is *P*2₁ or *P*2₁/*m*, and those from DL-MnC₄H₄O₆·2H₂O revealed that the space group is *Pc* or *P*2/*c*. Moreover, the intensity statistics of the reflections indicated that these crystals have non-centric or centric space groups. Thus, the space groups of the L- and DL-MnC₄H₄O₆·2H₂O crystals were determined to be monoclinic *P*2₁ and *P*2/*c*, respectively. Positional parameters for hydrogen atoms belonging to water molecules and isotropic thermal parameters of all hydrogen atoms for L-MnC₄H₄O₆·2H₂O were fixed in the structural refinements. The fixed hydrogen atoms were located on residual electron density peaks in the difference Fourier maps. Moreover, the thermal parameters of hydrogen atoms belonging to water molecules for DL-MnC₄H₄O₆·2H₂O were also fixed in the refinements. Final *R*-factors of 3.82% and 2.98% for the L- and DL-MnC₄H₄O₆·2H₂O crystals were calculated for 7156 and 3708 unique observed reflections, respectively.

Table 1. Crystal data, intensity data collections, and structure refinements for (a) L-MnC₄H₄O₆·2H₂O and (b) DL-MnC₄H₄O₆·2H₂O

	(a)	(b)
Compound, <i>M_r</i>	MnO ₈ C ₄ H ₈ , 239.04	MnO ₈ C ₄ H ₈ , 239.04
Measurement temperature	299 K	299 K
Crystal system, space group	Monoclinic, <i>P</i> 2 ₁	Monoclinic, <i>P</i> 2/ <i>c</i>
Lattice constants	<i>a</i> = 7.5901(2) Å <i>b</i> = 11.1883(2) Å <i>c</i> = 9.0076(3) Å <i>β</i> = 99.506(2) °	<i>a</i> = 11.0376(3) Å <i>b</i> = 7.3943(2) Å <i>c</i> = 10.1636(3) Å <i>β</i> = 112.167(1) °
V, Z	754.42(4) Å ³ , 4	768.19(4) Å ³ , 4
D(cal.)	2.105 Mg m ⁻³	2.067 Mg m ⁻³
<i>μ</i> (Mo <i>K_α</i>)	1.766 mm ⁻¹	1.734 mm ⁻¹
F(000)	484	484
Crystal size	0.12×0.20×0.20 mm ³	0.12×0.18×0.28 mm ³
<i>θ</i> range for data collection	2.72 – 38.04 °	1.99 – 37.97 °
Index ranges	-13≤ <i>h</i> ≤12, -19≤ <i>k</i> ≤19, -15≤ <i>l</i> ≤15	-19≤ <i>h</i> ≤19, -12≤ <i>k</i> ≤12, -17≤ <i>l</i> ≤17
Reflections collected, unique	21858, 7848 [<i>R</i> (int) = 0.0241]	21491, 4068 [<i>R</i> (int) = 0.0246]
Completeness to <i>θ</i> _{max}	97.1%	97.5 %
Absorption correction type	Numerical	Numerical
Transmission factor <i>T</i> _{min} – <i>T</i> _{max}	0.7141 – 0.8171	0.6756 – 0.8312
Date, parameter	7156 [<i>I</i> > 2σ(<i>I</i>)], 260	3708 [<i>I</i> > 2σ(<i>I</i>)], 147
Final <i>R</i> indices	<i>R</i> ₁ = 0.0382, <i>wR</i> ₂ = 0.0908	<i>R</i> ₁ = 0.0298, <i>wR</i> ₂ = 0.0678
<i>R</i> indices (all data)	<i>R</i> ₁ = 0.0439, <i>wR</i> ₂ = 0.0958	<i>R</i> ₁ = 0.0344, <i>wR</i> ₂ = 0.0704
Weighting scheme	<i>w</i> = 1/[σ ² (<i>F</i> _o ²)+(0.0430 <i>P</i>) ² +0.3846 <i>P</i>], <i>P</i> = (<i>F</i> _o ² +2 <i>F</i> _c ²)/3	<i>w</i> = 1/[σ ² (<i>F</i> _o ²)+(0.0291 <i>P</i>) ² +0.2348 <i>P</i>], <i>P</i> = (<i>F</i> _o ² +2 <i>F</i> _c ²)/3
Flack parameter	0.002(5)	
Goodness-of-fit on <i>F</i> ²	1.051	1.096
Extinction coefficient	0.007(2)	0.009(1)
Largest diff. peak and hole	0.692 and -0.510 eÅ ⁻³	0.495 and -0.520 eÅ ⁻³

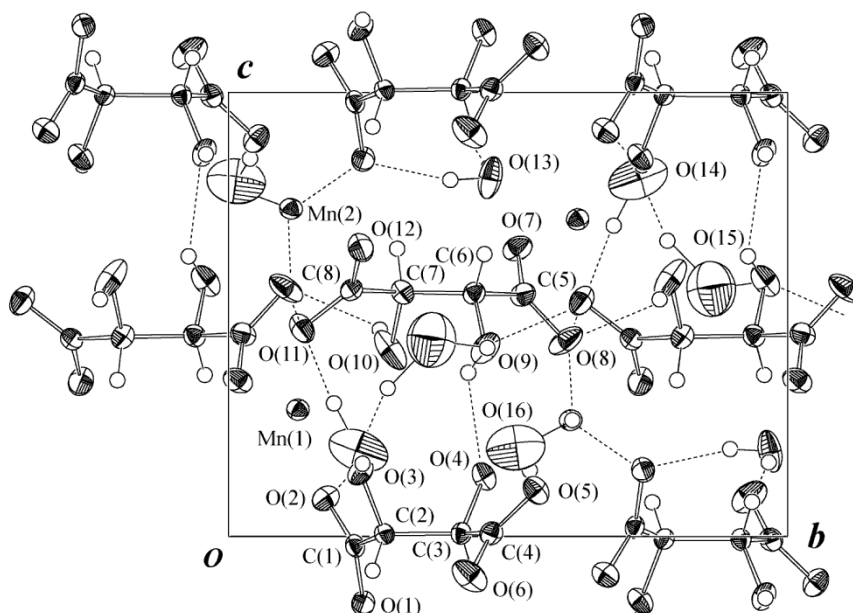
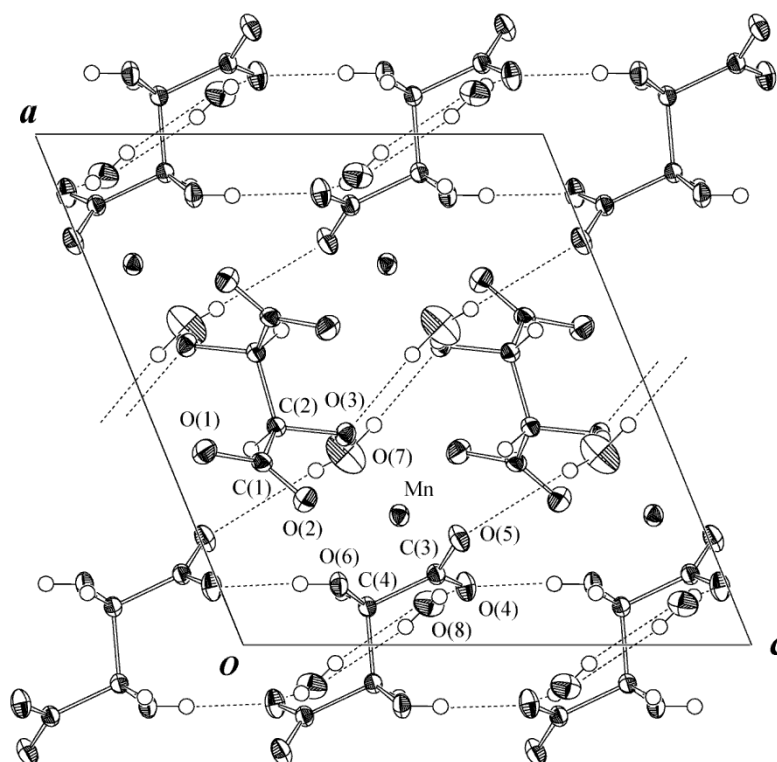
(a) L-MnC₄H₄O₆·2H₂O(b) DL-MnC₄H₄O₆·2H₂O

Figure 2. ORTEP projections along the *a*-axis of (a) L-MnC₄H₄O₆·2H₂O structure and in the *ac*-plane of (b) DL-MnC₄H₄O₆·2H₂O structure, with 50% probability-displacement thermal ellipsoids

The solid and dashed short lines indicate O-H···O hydrogen bonds, as shown in Table 4

Table 2. Atomic coordinates and thermal parameters ($\times 10^4 \text{ \AA}^2$) for (a) L-MnC₄H₄O₆·2H₂O and (b) DL-MnC₄H₄O₆·2H₂O at room temperature, with standard deviations in brackets. The anisotropic thermal parameters are defined as $\exp[-2\pi^2(U_{11}a^{*2}h^2 + U_{22}b^{*2}k^2 + U_{33}c^{*2}l^2 + 2U_{23}b^*c^*kl + 2U_{13}a^*c^*hl + 2U_{12}a^*b^*hk)]$. The isotropic thermal parameters (\AA^2) for H atoms are listed under U_{11}

(a) L-MnC ₄ H ₄ O ₆ ·2H ₂ O									
Atom	x	y	z	U_{11}	U_{22}	U_{33}	U_{23}	U_{13}	U_{12}
Mn(1)	0.14391(5)	0.12453(3)	0.28559(4)	199(2)	216(2)	193(1)	-1(1)	13(1)	-6(1)
Mn(2)	0.72928(5)	0.11224(3)	0.73813(4)	205(2)	224(2)	182(1)	-6(1)	7(1)	-29(2)
C(1)	0.0086(3)	0.2267(2)	-0.0211(3)	199(10)	157(8)	217(10)	-22(7)	-12(8)	-9(7)
C(2)	0.1964(3)	0.2792(2)	0.0056(3)	195(10)	171(9)	181(9)	-12(7)	26(8)	-19(7)
C(3)	0.1872(3)	0.4163(2)	0.0069(3)	182(9)	170(9)	205(10)	7(7)	24(8)	-12(7)
C(4)	0.3727(4)	0.4703(2)	0.0072(3)	218(11)	226(10)	226(11)	19(8)	66(8)	-38(9)
C(5)	0.1458(4)	0.5269(3)	0.5447(3)	276(12)	263(11)	225(11)	29(9)	65(9)	106(10)
C(6)	0.3020(4)	0.4396(2)	0.5478(3)	209(10)	205(10)	215(10)	16(8)	35(8)	22(8)
C(7)	0.2363(4)	0.3117(3)	0.5501(3)	220(11)	224(11)	244(11)	-32(9)	32(9)	-5(9)
C(8)	0.3863(4)	0.2202(2)	0.5555(3)	248(11)	207(10)	199(10)	24(8)	-8(8)	32(8)
O(1)	-0.0829(3)	0.2414(2)	-0.1501(2)	279(10)	220(8)	252(9)	11(7)	-81(7)	-45(7)
O(2)	-0.0446(3)	0.1744(2)	0.0859(2)	192(8)	308(10)	261(9)	55(8)	-9(7)	-55(7)
O(3)	0.2884(3)	0.2365(2)	0.1450(2)	167(8)	270(9)	276(9)	84(7)	-19(7)	-13(7)
O(4)	0.1164(3)	0.4573(2)	0.1352(3)	193(8)	239(9)	318(10)	-71(8)	87(7)	-22(7)
O(5)	0.4271(3)	0.5503(2)	0.1040(3)	226(9)	280(10)	327(11)	-74(8)	71(8)	-76(7)
O(6)	0.4562(4)	0.4315(3)	-0.0888(3)	407(14)	509(16)	431(14)	-180(12)	265(12)	-182(12)
O(7)	0.0576(4)	0.5172(2)	0.6487(3)	384(12)	359(11)	260(10)	68(8)	164(9)	139(10)
O(8)	0.1178(4)	0.6032(3)	0.4408(3)	513(14)	474(15)	333(10)	208(11)	224(10)	315(13)
O(9)	0.3918(4)	0.4599(2)	0.4243(3)	320(12)	346(12)	402(13)	142(10)	194(10)	119(10)
O(10)	0.1032(3)	0.2902(3)	0.4199(4)	214(10)	434(14)	639(19)	-310(13)	-131(11)	116(10)
O(11)	0.3610(3)	0.1317(2)	0.4688(3)	347(10)	258(10)	347(10)	-92(9)	-129(8)	112(9)
O(12)	0.5241(3)	0.2369(2)	0.6508(3)	336(11)	268(10)	334(11)	-41(8)	-137(9)	75(8)
O(13)	0.7563(4)	0.4683(2)	0.8082(4)	296(11)	240(10)	740(20)	120(12)	236(12)	21(9)
O(14)	0.3674(5)	0.7326(6)	0.8060(5)	292(15)	1463(48)	761(28)	309(30)	76(16)	-226(22)
O(15)	0.2337(9)	0.8632(7)	0.5574(8)	938(44)	1003(45)	1275(52)	-34(41)	181(40)	101(36)
O(16)	0.7864(5)	0.5140(6)	0.2001(6)	313(17)	1438(52)	853(32)	72(33)	-89(18)	3(24)
H(1)	0.269(6)	0.258(4)	-0.077(5)	0.03					
H(2)	0.119(6)	0.436(4)	-0.078(5)	0.03					
H(3)	0.416(6)	0.458(4)	0.636(5)	0.03					
H(4)	0.195(6)	0.302(4)	0.648(5)	0.03					
H(5)	0.407(8)	0.240(5)	0.164(6)	0.05					
H(6)	0.022(8)	0.460(6)	0.139(6)	0.05					
H(7)	0.334(8)	0.429(6)	0.369(7)	0.05					
H(8)	0.030(9)	0.271(5)	0.466(6)	0.05					
H(9)	0.803	0.398	0.804	0.07					
H(10)	0.656	0.466	0.833	0.07					
H(11)	0.275	0.731	0.860	0.07					
H(12)	0.341	0.690	0.701	0.07					
H(13)	0.221	0.964	0.575	0.07					
H(14)	0.348	0.785	0.666	0.07					
H(15)	0.684	0.539	0.150	0.07					
H(16)	0.869	0.616	0.263	0.07					
(b) DL-MnC ₄ H ₄ O ₆ ·2H ₂ O									
Mn	x	y	z	U_{11}	U_{22}	U_{33}	U_{23}	U_{13}	U_{12}
Mn	0.25419(2)	0.85236(2)	0.41130(2)	206.3(7)	189.1(7)	165.3(7)	-31.2(5)	71.5(5)	-32.6(5)
C(1)	0.35819(9)	0.9234(1)	0.1833(1)	158(3)	221(4)	172(4)	49(3)	40(3)	1(3)
C(2)	0.42723(9)	0.7442(1)	0.24032(9)	163(3)	185(3)	149(3)	9(3)	51(3)	-5(3)
C(3)	0.13888(9)	0.4964(1)	0.43628(9)	180(3)	186(3)	137(3)	10(3)	55(3)	17(3)
C(4)	0.07509(8)	0.5188(1)	0.27480(9)	169(3)	166(3)	131(3)	-1(3)	53(3)	-7(3)
O(1)	0.37872(8)	0.9877(1)	0.07904(9)	261(4)	412(5)	279(4)	198(3)	136(3)	113(3)
O(2)	0.28528(8)	0.9917(1)	0.23904(8)	268(3)	209(3)	257(3)	43(3)	129(3)	41(3)
O(3)	0.41284(7)	0.6988(1)	0.37011(8)	229(3)	198(3)	198(3)	51(2)	103(3)	15(2)
O(4)	0.11457(9)	0.3499(1)	0.48456(8)	355(4)	182(3)	168(3)	23(2)	97(3)	-7(3)
O(5)	0.20908(8)	0.6198(1)	0.51038(8)	298(4)	251(3)	143(3)	-6(2)	38(3)	-69(3)

O(6)	0.11888(8)	0.6828(1)	0.23677(8)	255(3)	223(3)	138(3)	-12(2)	80(2)	-78(2)
O(7)	0.3743(2)	0.3472(1)	0.3551(2)	643(8)	244(4)	471(7)	-41(4)	9(6)	-17(4)
O(8)	0.08081(9)	0.0103(1)	0.3982(1)	271(4)	252(4)	342(4)	-76(3)	67(3)	0(3)
H(1)	0.384(1)	0.659(2)	0.172(2)	0.018(3)					
H(2)	0.102(1)	0.416(2)	0.235(1)	0.018(3)					
H(3)	0.405(2)	0.594(3)	0.373(2)	0.046(5)					
H(4)	0.120(2)	0.672(3)	0.161(2)	0.053(6)					
H(5)	0.342(3)	0.308(4)	0.283(3)	0.07					
H(6)	0.431(3)	0.280(4)	0.434(3)	0.07					
H(7)	0.095(3)	0.122(4)	0.425(3)	0.07					
H(8)	0.036(3)	0.005(3)	0.334(2)	0.07					

The relevant crystal data, and a summary of the intensity data collections and structure refinement parameters are given in Table 1. Figure 2 shows the projections of the L-MnC₄H₄O₆·2H₂O crystal structure along the *a*-axis and of the DL-MnC₄H₄O₆·2H₂O crystal structure on the *ac*-plane. The positional parameters in fractions of the unit cell and the thermal parameters are listed in Table 2. Selected bond lengths and angles are given in Table 3, and hydrogen-bond geometries are presented in Table 4.

3.2 Structure Description

The observed lattice constants of L-MnC₄H₄O₆·2H₂O differ from those of MnC₄H₄O₆·4H₂O previously reported by Soylu (Soylu, 1985), and are very close to those of MnC₄H₄O₆·2H₂O reported by Labutina et al (Labutina, Marychev, Portnov, Somov, & Chuprunov, 2011). This difference is considered to be attributed to the difference in the number of bound water molecules contained in the crystals. The observed unit cell structure consists of two non-equivalent Mn atoms, two crystallographically independent C₄H₄O₆ molecules, and four independent H₂O molecules. It is seen from Fig. 2(a) of L-MnC₄H₄O₆·2H₂O that the C₄H₄O₆ and H₂O ligands are located near the (001)- and (002)-planes perpendicular to the *c*-axis, and Mn atoms are situated between these planes. Moreover, the Mn atoms are bonded to six nearest-neighboring O atoms, forming slightly distorted MnO₆ octahedra. The six atoms bonding to the Mn(1) atom are five O atoms from three C₄H₄O₆ molecules and one O atom from the H₂O molecule, and the atoms bonding to the Mn(2) atom are also six O atoms from four C₄H₄O₆ molecules, as shown in Table 3(a). Therefore, the three C₄H₄O₆ molecules and one H₂O molecule are connected to each other through the Mn(1)–O bonds, and the four C₄H₄O₆ molecules are also connected to each other through the Mn(2)–O bonds. The lengths of the Mn–O bonds are in the range of 2.105(2)–2.334(3) Å, and the average Mn–O distance is 2.182 Å.

On the other hand, the unit cell structure of DL-MnC₄H₄O₆·2H₂O consists of one type of Mn atom, two crystallographically independent C₄H₄O₆ molecules, and two independent H₂O molecules. The Mn atom is also bonded to six nearest-neighboring O atoms, forming a slightly distorted MnO₆ octahedron. The six atoms are five O atoms from three C₄H₄O₆ molecules and one O atom from the H₂O molecule. Thus, the three C₄H₄O₆ molecules and one H₂O molecule are connected to each other through the Mn–O bonds. The lengths of the Mn–O bonds are in the range of 2.1037(8)–2.2248(7) Å, and the average Mn–O distance is 2.183 Å. The Mn–O distance and MnO₆ octahedron shape in DL-MnC₄H₄O₆·2H₂O are similar to those in L-MnC₄H₄O₆·2H₂O.

The magnitudes of the thermal parameters for the O atoms (O(14)–O(16) in Table 2(a), and O(7) in Table 2(b)) in the H₂O molecules of both crystals that are not bonded to any atoms are larger than those for the O atoms (O(13) in Table 2(a), and O(8) in Table 2(b)) bonded to the Mn atom, as shown in Table 2 and Fig. 2. The thermal parameters, more formally termed atomic displacement parameters, relate to the magnitudes and directions of the thermal vibration of atoms. This indicates that the thermal vibrations of the O atoms are strongly affected by the bonding strength between the Mn and O atoms.

The C₄H₄O₆ and H₂O molecules located near the (001)- and (002)-planes as shown in Fig. 2(a) of L-MnC₄H₄O₆·2H₂O are connected to each other by O–H–O hydrogen bonds. Moreover, it is observed that the zig-zag hydrogen-bonding networks along the *a*-, *b*- and *c*-axes are constructed by linking the molecules through the hydrogen bonds. On the other hand, three hydrogen-bonded chains can be clearly seen in the DL-MnC₄H₄O₆·2H₂O structure of Fig. 2(b). Two equivalent chains lie along the *c*-axis, which consist of C₄H₄O₆ molecules connected through two equivalent O(6)–H(4)··O(4) hydrogen bonds. The remaining chain runs along the [201]-direction, which is also constructed from C₄H₄O₆ and H₂O molecules through O(7)–H(5)··O(5) and O(7)–H(6)··O(3) hydrogen bonds.

Table 3. Selected interatomic distances (in Å) and angles (in degrees) for (a) L-MnC₄H₄O₆·2H₂O and (b) DL-MnC₄H₄O₆·2H₂O

(a) L-MnC ₄ H ₄ O ₆ ·2H ₂ O			
Mn(1)–O(2)	2.178(2)	Mn(1)–O(3)	2.199(2)
Mn(1)–O(7) ⁽¹⁾	2.105(2)	Mn(1)–O(10)	2.263(3)
Mn(1)–O(11)	2.132(2)	Mn(1)–O(13) ⁽²⁾	2.134(3)
Mn(2)–O(1) ⁽³⁾	2.159(2)	Mn(2)–O(4) ⁽²⁾	2.289(2)
Mn(2)–O(5) ⁽²⁾	2.114(2)	Mn(2)–O(8) ⁽²⁾	2.139(2)
Mn(2)–O(9) ⁽²⁾	2.334(3)	Mn(2)–O(12)	2.141(2)
O(1)–C(1)	1.262(3)	O(2)–C(1)	1.250(3)
O(3)–C(2)	1.415(3)	O(4)–C(3)	1.428(3)
O(5)–C(4)	1.271(3)	O(6)–C(4)	1.232(4)
O(7)–C(5)	1.243(4)	O(8)–C(5)	1.258(4)
O(9)–C(6)	1.415(4)	O(10)–C(7)	1.436(4)
O(11)–C(8)	1.256(4)	O(12)–C(8)	1.252(3)
C(1)–C(2)	1.524(4)	C(2)–C(3)	1.536(4)
C(3)–C(4)	1.531(4)	C(5)–C(6)	1.533(4)
C(6)–C(7)	1.516(4)	C(7)–C(8)	1.526(4)
O(1)–C(1)–O(2)	124.9(2)	O(1)–C(1)–C(2)	117.0(2)
O(2)–C(1)–C(2)	118.1(2)	O(3)–C(2)–C(1)	108.8(2)
O(3)–C(2)–C(3)	110.3(2)	O(4)–C(3)–C(2)	110.5(2)
O(4)–C(3)–C(4)	109.9(2)	O(5)–C(4)–C(3)	118.3(2)
O(6)–C(4)–O(5)	125.6(3)	O(6)–C(4)–C(3)	116.1(3)
O(7)–C(5)–O(8)	125.0(3)	O(7)–C(5)–C(6)	116.2(2)
O(8)–C(5)–C(6)	118.8(2)	O(9)–C(6)–C(5)	110.8(2)
O(9)–C(6)–C(7)	111.4(2)	O(10)–C(7)–C(6)	109.6(3)
O(10)–C(7)–C(8)	109.5(2)	O(11)–C(8)–C(7)	118.2(2)
O(12)–C(8)–O(11)	124.6(3)	O(12)–C(8)–C(7)	117.2(2)
C(1)–C(2)–C(3)	110.1(2)	C(2)–C(3)–C(4)	110.5(2)
C(5)–C(6)–C(7)	110.3(2)	C(6)–C(7)–C(8)	112.8(2)
(b) DL-MnC ₄ H ₄ O ₆ ·2H ₂ O			
Mn–O(1) ⁽⁴⁾	2.1037(8)	Mn–O(2)	2.1676(8)
Mn–O(3)	2.2548(8)	Mn–O(5)	2.1443(8)
Mn–O(6)	2.2248(7)	Mn–O(8) ⁽⁵⁾	2.2026(9)
O(1)–C(1)	1.258(1)	O(2)–C(1)	1.252(1)
O(3)–C(2)	1.427(1)	O(4)–C(3)	1.259(1)
O(5)–C(3)	1.249(1)	O(6)–C(4)	1.413(1)
C(1)–C(2)	1.529(1)	C(2)–C(2) ⁽⁶⁾	1.543(2)
C(3)–C(4)	1.531(1)	C(4)–C(4) ⁽⁷⁾	1.540(2)
O(1)–C(1)–O(2)	125.41(9)	O(1)–C(1)–C(2)	115.11(9)
O(2)–C(1)–C(2)	119.46(8)	O(3)–C(2)–C(1)	109.92(7)
O(3)–C(2)–C(2) ⁽⁶⁾	110.84(9)	O(4)–C(3)–O(5)	124.64(9)
O(4)–C(3)–C(4)	115.55(8)	O(5)–C(3)–C(4)	119.81(8)
O(6)–C(4)–C(3)	108.65(7)	O(6)–C(4)–C(4) ⁽⁷⁾	110.34(6)
C(1)–C(2)–C(2) ⁽⁶⁾	113.23(5)	C(3)–C(4)–C(4) ⁽⁷⁾	110.72(9)

Symmetry codes: (1) $-x, y-1/2, -z+1$; (2) $-x+1, y-1/2, -z+1$; (3) $x+1, y, z+1$; (4) $x, -y+2, z+1/2$; (5) $x, y+1, z$; (6) $-x+1, y, -z+1/2$; (7) $-x, y, -z+1/2$.

Table 4. Selected hydrogen bond distances (in Å) and angles (in degrees) for (a) L-MnC₄H₄O₆·2H₂O and (b) DL-MnC₄H₄O₆·2H₂O

	D–H··A	D–H	H··A	D··A	<D–H··A
(a)	C(2)–H(1)	1.02(5)			
	C(3)–H(2)	0.88(5)			
	C(6)–H(3)··O(13)	1.10(5)	2.79(5)	3.850(4)	164(3)
	C(7)–H(4)	0.99(4)			
	O(3)–H(5)··O(14) ⁽¹⁾	0.89(6)	1.69(6)	2.576(4)	174(6)
	O(4)–H(6)··O(16) ⁽²⁾	0.73(6)	2.04(6)	2.739(5)	161(6)
	O(9)–H(7)··O(4)	0.70(6)	2.47(6)	3.059(4)	142(7)
	O(10)–H(8)··O(8) ⁽³⁾	0.78(6)	2.41(6)	3.076(5)	145(6)
	O(13)–H(9)··O(1) ⁽⁴⁾	0.870(3)	1.966(2)	2.815(3)	165.1(2)
	O(13)–H(10)··O(6) ⁽⁵⁾	0.827(3)	1.818(2)	2.630(4)	167.2(2)
	O(14)–H(11)··O(2) ⁽⁶⁾	0.913(4)	2.000(2)	2.857(4)	156.0(4)
	O(14)–H(12)··O(8)	1.053(6)	2.824(3)	3.801(6)	154.4(2)
	O(15)–H(13)··O(11) ⁽⁷⁾	1.145(7)	2.429(3)	3.294(8)	130.9(4)
	O(15)–H(14)··O(14)	1.479(7)	1.375(5)	2.725(9)	145.4(3)
	O(16)–H(15)··O(5)	0.879(4)	1.931(2)	2.752(4)	154.8(4)
	O(16)–H(16)··O(1) ⁽⁸⁾	1.374(6)	2.488(3)	3.475(6)	125.8(2)
O(16)–H(16)··O(8) ⁽⁹⁾	1.374(6)	2.273(3)	3.197(6)	120.5(2)	
(b)	C(2)–H(1)··O(5) ⁽¹⁰⁾	0.92(1)	2.88(2)	3.776(1)	164(1)
	C(4)–H(2)··O(5) ⁽¹⁰⁾	0.96(1)	2.96(1)	3.669(1)	132(1)
	O(3)–H(3)··O(7)	0.78(2)	1.85(2)	2.630(1)	173(2)
	O(6)–H(4)··O(4) ⁽¹⁰⁾	0.78(2)	1.78(2)	2.557(1)	177(2)
	O(7)–H(5)··O(5) ⁽¹⁰⁾	0.74(2)	2.65(3)	3.292(2)	146(3)
	O(7)–H(6)··O(3) ⁽¹¹⁾	0.95(3)	2.09(3)	2.913(2)	144(2)
	O(8)–H(7)··O(4)	0.87(3)	1.77(3)	2.640(1)	176(3)
	O(8)–H(8)··O(8) ⁽¹²⁾	0.66(2)	2.22(2)	2.864(2)	167(3)

Symmetry codes: (1) $-x+1, y-1/2, -z+1$; (2) $x-1, y, z$; (3) $-x, y-1/2, -z+1$; (4) $x+1, y, z+1$; (5) $x, y, z+1$; (6) $-x, y+1/2, -z+1$; (7) $x, y+1, z$; (8) $-x+1, y+1/2, -z$; (9) $x+1, y, z$; (10) $x, -y+1, z-1/2$; (11) $-x+1, -y+1, -z+1$; (12) $-x, y, -z+1/2$.

The lengths of O–C bonds in the C₄H₄O₆ molecules of L-MnC₄H₄O₆·2H₂O and DL-MnC₄H₄O₆·2H₂O are in the range of 1.232(4)–1.436(4) Å and 1.252(1)–1.427(1) Å, respectively. The variation in the O–C distances is probably related to differences in bond type. The lengths of single and double O–C bonds in organic molecules are respectively around 1.43 and 1.22 Å, and the length of C–C single bonds is around 1.54 Å. Therefore, the two O–C bonds of hydroxyl groups in the C₄H₄O₆ molecule of both crystals have single-bond character, and the remaining four bonds have double-bond character. The lengths of C–C bonds in L-MnC₄H₄O₆·2H₂O and DL-MnC₄H₄O₆·2H₂O are in the range of 1.516(4)–1.536(4) Å and 1.529(1)–1.543(1) Å, respectively, indicating that all the C–C bonds have a single-bond character. The angles between the two least-squares planes of atoms, [C(1)C(2)O(1)O(2)O(3)] and [C(3)C(4)O(4)O(5)O(6)], and [C(5)C(6)O(7)O(8)O(9)] and [C(7)C(8)O(10)O(11)O(12)], in the C₄H₄O₆ molecules of L-MnC₄H₄O₆·2H₂O were calculated to be 58.0(1)° and 74.6(1)°, respectively. Moreover, the angles between the planes [C(1)C(2)O(1)O(2)O(3)] and [C(1)C(2)O(1)O(2)O(3)] and [C(3)C(4)O(4)O(5)O(6)] and [C(3)C(4)O(4)O(5)O(6)] in the molecules of DL-MnC₄H₄O₆·2H₂O were also calculated to be 65.71(4)° and 51.39(3)°, respectively. The angles in DL-MnC₄H₄O₆·2H₂O are smaller (about 8°) than those in L-MnC₄H₄O₆·2H₂O, comparing the closing values of the angle.

Comparing the C₄H₄O₆ molecules in both crystals shown in Table 3, it is seen that the structures of the four molecules in the crystals are similar to each other, except for the differences in the plane angle. However, it is noticed from Fig. 2(b) that the C₄H₄O₆ molecule in DL-MnC₄H₄O₆·2H₂O, which consists of C(1)C(2)O(1)O(2)O(3), has a cis-like-form, and the other three molecules have a trans-like-form. This result indicates that there is no geometrical chirality between the C₄H₄O₆ molecules in the DL-MnC₄H₄O₆·2H₂O crystal. Moreover, one of the C₄H₄O₆ molecules in DL-tartaric acid is presumed to vary from the trans-like-form to the cis-like-form during the growth of the DL-MnC₄H₄O₆·2H₂O crystals,

because DL-tartaric acid is a mixture of L-tartaric and D-tartaric acid (relating to mirror symmetry) in the same amount, and the $C_4H_6O_6$ molecules in the DL-tartaric acid crystal have the trans-like-form (Fukami, Tahara, Yasuda, & Nakasone, 2016). The $C_4H_4O_6$ molecule having the cis-like-form has not been found in the crystal structures of other tartaric salts (Fukami, Hiyajyo, Tahara, & Yasuda, 2017a; Fukami, Hiyajyo, Tahara, & Yasuda, 2017b; Fukami, & Tahara, 2018; Fukami, Tahara, Yasuda, & Nakasone, 2016; Song, Teng, Dong, Ma, & Sun, 2006).

3.3 Thermal Analysis

Figure 3 shows the TG, differential TG (DTG), and DTA curves for the L- and DL- $MnC_4H_4O_6 \cdot 2H_2O$ crystals in the temperature range of 300–1470 K. The sample weights (powder) of the L- and DL- $MnC_4H_4O_6 \cdot 2H_2O$ crystals used for the measurements were 4.03 and 4.94 mg, respectively. The heating rate was 10 K min^{-1} under a dry nitrogen gas flow of 300 ml min^{-1} . The observed TG curve of L- $MnC_4H_4O_6 \cdot 2H_2O$ is very similar to that in the published paper by Yanes et al (Yanes, Lopez, Stockel, Peraza, & Torres, 1996). The DTA curve of L- $MnC_4H_4O_6 \cdot 2H_2O$ shows three apparent endothermic peaks at 354, 629, 666 K including a small peak, and the DTG curve shows three peaks at 352, 631, 678 K. On the other hand, three endothermic peaks at 406, 612, and 662 K are observed in the DTA curve of DL- $MnC_4H_4O_6 \cdot 2H_2O$, and moreover, three peaks at 404, 611, and 671 K are also found in the DTG curve. The endothermic peak temperatures on the DTA curves of both crystals are very close to those on the DTG curves. The DTG curve, which is the first derivative of TG curve, reveals the temperature dependence of weight loss rate due to thermal decomposition of sample. Thus, the DTA peaks are associated with the maximum rate of weight loss in the TG curve. DSC measurements on the powder samples of both crystals were performed in the temperature range from 100 to 310 K at a heating rate of 10 K min^{-1} . No obvious endothermic or exothermic peaks were observed in the temperature range, except for small changes of the baseline in the curves due to the endothermic peaks at 354 or 406 K. In general, it is believed that a clear peak in DSC (or DTA) curve is attributed to the change in exchange energy at phase transition. Thus, the obtained results indicate that there is no phase transition in the temperature range of 100–310 K in both the crystals.

Table 5. TG results for thermal decomposition of (a) L- $MnC_4H_4O_6 \cdot 2H_2O$ and (b) DL- $MnC_4H_4O_6 \cdot 2H_2O$

Temp. range [K]	(a)	(b)	Theoretical loss (cal.) [%]	Elimination molecules
	Weight loss (obs.) [%]	Weight loss (obs.) [%]		
300–490	13.6	15.7	15.1	$2H_2O$
490–760	51.2	50.2	48.6	$C_4H_4O_4$
760–1150	7.7	7.4	6.7	$(1/2)O_2$
Total	72.5	73.3	70.4	

Two large weight losses in the TG curves for both crystals are seen at around 350 K and 650 K. The weight losses of L- $MnC_4H_4O_6 \cdot 2H_2O$ in the temperature ranges of 300–490, 490–760 and 760–1150 K were found to be 13.6, 51.2, and 7.7%, and of DL- $MnC_4H_4O_6 \cdot 2H_2O$ to be 15.7, 50.2, and 7.4%, respectively, as described in Fig. 3. Table 5 shows the experimental and theoretical (calculated based on following considerations) weight losses in each temperature range.

The weight losses in the TG curve are thought to be caused by the evolution of gases from the sample, similar to previous reports (Fukami, Hiyajyo, Tahara, & Yasuda, 2017a; Fukami, Hiyajyo, Tahara, & Yasuda, 2017b; Fukami & Tahara, 2018; Fukami, Tahara, Yasuda, & Nakasone, 2016). We assume that two bound H_2O molecules within the crystals (having the same chemical formula) are evaporated with increasing temperature. The theoretical weight loss due to the evaporation of $2H_2O$ is calculated to be 15.1 % ($=2 \times 18.0 / 239.04$). This calculated value is almost close to the experimental loss values (13.6 and 15.7%) in the range of 300–490 K. Moreover, we assume that the crystals are decomposed to $C_4H_4O_4$ and MnO_2 molecules in the temperature range of 490–760 K, and the weight losses are caused by the evolution of gases from $C_4H_4O_4$. The theoretical weight loss due to the evaporation of the gases is calculated to be 48.6% ($=116.07 / 239.04$), and is found to be close to the experimental loss values (51.2 and 50.2%) in the range of 490–760 K. It is found that the inflection points on both the TG curves of Fig. 3 appear at around 650 K, and moreover, are close to a respective center of the weight losses in the range of 490–760 K. These results reveal that the weight losses due to the evolution of gases in this range are caused by two decomposition processes of $C_4H_4O_4$, and the evolved gases are presumed to be $2H_2CO$ and $2CO$. Unfortunately, since the thermal loss processes in the TG curves at around 650 K are observed over narrow temperature ranges, detailed information of the processes can not be obtained.

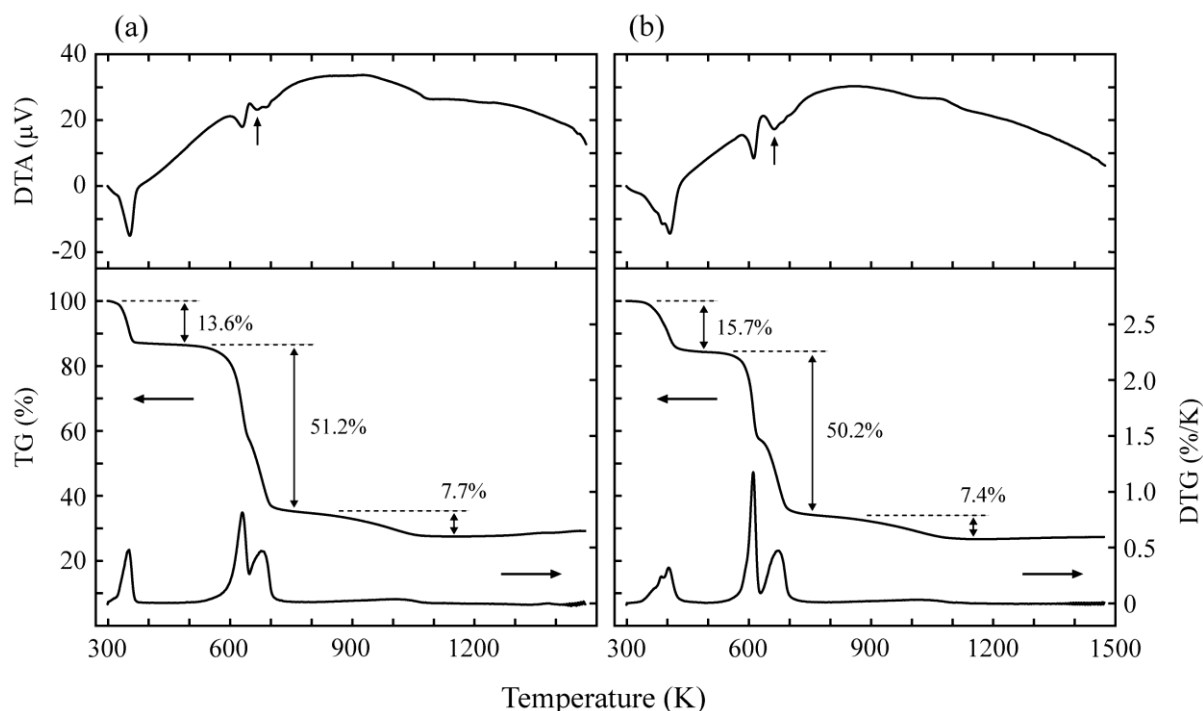


Figure 3. TG, DTG, and DTA curves for (a) L- $\text{MnC}_4\text{H}_4\text{O}_6 \cdot 2\text{H}_2\text{O}$ and (b) DL- $\text{MnC}_4\text{H}_4\text{O}_6 \cdot 2\text{H}_2\text{O}$ crystals on heating

Lastly, we assume that the weight loss in the range of 760–1150 K is produced by the evolution of $(1/2)\text{O}_2$ gas from MnO_2 . The theoretical weight loss is calculated to be 6.7% ($=16.00 / 239.04$). This value is very close to the experimental loss values of 7.7 and 7.4% in the range of 760–1150 K. The total experimental weight losses of the L- and DL- $\text{MnC}_4\text{H}_4\text{O}_6 \cdot 2\text{H}_2\text{O}$ crystals in the range of 300–1150 K are 72.5% ($=13.6 + 51.2 + 7.7\%$) and 73.3% ($=15.7 + 50.2 + 7.4\%$), respectively. These values are close to the total theoretical weight loss of 70.4% ($=15.1 + 48.6 + 6.7\%$). After heating up to 1470 K for the TG-DTA measurements of both crystals, we found that small black materials were present in the respective vessels. The residual materials from the samples are presumed to be manganese oxide MnO .

4. Summary

Crystals of L- $\text{MnC}_4\text{H}_4\text{O}_6 \cdot 2\text{H}_2\text{O}$ and DL- $\text{MnC}_4\text{H}_4\text{O}_6 \cdot 2\text{H}_2\text{O}$ were grown in silica gel medium at room temperature by the diffusion method. The structures and thermal properties of these crystals were studied by means of X-ray diffraction, DSC, and TG-DTA. The room-temperature crystal structures of L- $\text{MnC}_4\text{H}_4\text{O}_6 \cdot 2\text{H}_2\text{O}$ and DL- $\text{MnC}_4\text{H}_4\text{O}_6 \cdot 2\text{H}_2\text{O}$ were determined to be monoclinic with space groups $P2_1$ and $P2/c$, respectively. The determined structures consisted of slightly distorted MnO_6 octahedra, $\text{C}_4\text{H}_4\text{O}_6$ and H_2O molecules, and stabilization by $\text{O}-\text{H} \cdots \text{O}$ hydrogen bonds between adjacent $\text{C}_4\text{H}_4\text{O}_6$ or H_2O molecules. It was confirmed that there is no geometrical chirality between the $\text{C}_4\text{H}_4\text{O}_6$ molecules in the DL- $\text{MnC}_4\text{H}_4\text{O}_6 \cdot 2\text{H}_2\text{O}$ crystal. In both crystals, no phase transition was observed in the temperature range of 100–310 K, and the weight losses due to thermal decomposition were found to occur in the temperature range of 300–1150 K. We suggested that the weight losses are caused by the evaporation of bound $2\text{H}_2\text{O}$ molecules, and the evolutions of gases from $\text{C}_4\text{H}_4\text{O}_4$ and of $(1/2)\text{O}_2$ gas from MnO_2 , and that the residual black substance in vessels after decomposition is manganese oxide MnO .

References

- Abdel-Kader, M. M., El-Kabbany, F., Taha, S., Abosehly, A. M., Tahoon, K. K., & El-Sharkawy, A. A. (1991). Thermal and electrical properties of ammonium tartrate. *J. Phys. Chem. Solids*, *52*(5), 655-658. [https://doi.org/10.1016/0022-3697\(91\)90163-T](https://doi.org/10.1016/0022-3697(91)90163-T)
- Bootsma, G. A., & Schoone, J. C. (1967). Crystal structures of mesotartaric acid. *Acta Crystallogr.*, *22*(4), 522-532. <https://doi.org/10.1107/S0365110X67001070>
- Burla, M. C., Caliandro, R., Camalli, M., Carrozzini, B., Cascarano, G. L., Giacovazzo, C., ... Spagna, R. (2012). SIR2011: a new package for crystal structure determination and refinement. *J. Appl. Crystallogr.*, *45*(2), 357-361. <https://doi.org/10.1107/S0021889812001124>

- Desai, C. C., & Patel, A. H. (1988). Crystal data for ferroelectric $\text{RbHC}_4\text{H}_4\text{O}_6$ and $\text{NH}_4\text{HC}_4\text{H}_4\text{O}_6$ crystals. *J. Mater. Sci. Lett.*, 7(4), 371-373. <https://doi.org/10.1007/BF01730747>
- Farrugia, L. J. (2012). WinGX and ORTEP for Windows: an update. *J. Appl. Crystallogr.*, 45(4), 849-854. <https://doi.org/10.1107/S0021889812029111>
- Firdous, A., Quasim, I., Ahmad, M. M., & Kotru, P. N. (2010). Dielectric and thermal studies on gel grown strontium tartrate pentahydrate crystals. *Bull. Mater. Sci.*, 33(4), 377-382. <https://doi.org/10.1007/s12034-010-0057-1>
- Fukami, T., & Tahara, S. (2018). Structural and thermal studies on racemic $\text{PbC}_4\text{H}_4\text{O}_6 \cdot 2\text{H}_2\text{O}$ single crystal. *Chem. Sci. Int. J.*, 25(1), 45004(1-9). <https://doi.org/10.9734/CSJI/2018/45004>
- Fukami, T., Hiyajyo, S., Tahara, S., & Yasuda, C. (2017a). Thermal properties and crystal structure of $\text{BaC}_4\text{H}_4\text{O}_6$ single crystals. *Inter. J. Chem.*, 9(1), 30-37. <https://doi.org/10.5539/ijc.v9n1p30>
- Fukami, T., Hiyajyo, S., Tahara, S., & Yasuda, C. (2017b). Crystal structure and thermal properties of racemic $\text{SrC}_4\text{H}_4\text{O}_6 \cdot 4\text{H}_2\text{O}$ single crystals. *Inter. Res. J. Pure Appl. Chem.*, 14(2), 34299(1-10). <https://doi.org/10.9734/IRJPAC/2017/34299>
- Fukami, T., Tahara, S., Yasuda, C., & Nakasone, K. (2016). Structural refinements and thermal properties of L(+)-tartaric, D(-)-tartaric, and monohydrate racemic tartaric acid. *Inter. J. Chem.*, 8(2), 9-21. <https://doi.org/10.5539/ijc.v8n2p9>
- Labutina, M. L., Marychev, M. O., Portnov, V. N., Somov, N. V., & Chuprunov, E. V. (2011). Second-order nonlinear susceptibilities of the crystals of some metal tartrates. *Crystallogr. Rep.*, 56(1), 72-74. <https://doi.org/10.1134/S1063774510061082>
- Sheldrick, G. M. (2015). Crystal structure refinement with SHELXL. *Acta Crystallogr.*, C71(1), 3-8. <https://doi.org/10.1107/S2053229614024218>
- Song, Q. B., Teng, M. Y., Dong, Y., Ma, C. A., & Sun, J. (2006). (2S,3S)-2,3-Dihydroxy-succinic acid monohydrate. *Acta Crystallogr.*, E62(8), o3378-o3379. <https://doi.org/10.1107/S1600536806021738>
- Soylu, H. (1985). The crystal structure of manganese (II) L-tartrate tetrahydrate $\text{MnC}_4\text{H}_4\text{O}_6 \cdot 4\text{H}_2\text{O}$. *Z. Kristallogr.*, 171(1-4), 255-260. <https://doi.org/10.1524/zkri.1985.171.14.255>
- Torres, M. E., Peraza, J., Yanes, A. C., López, T., Stockel, J., López, D. M., ... Silgo, G. G. (2002). Electrical conductivity of doped and undoped calcium tartrate. *J. Phys. Chem. Solids*, 63(4), 695-698. [https://doi.org/10.1016/S0022-3697\(01\)00216-5](https://doi.org/10.1016/S0022-3697(01)00216-5)
- Yanes, A. C., Lopez, T., Stockel, J., Peraza, J. F., & Torres, M. E. (1996). Characterization and thermal and electromagnetic behaviour of manganese tartrate crystals grown by the silica gel technique. *J. Mater. Sci.*, 31(10), 2683-2686. <https://doi.org/10.1007/BF00687300>

Copyrights

Copyright for this article is retained by the author(s), with first publication rights granted to the journal.

This is an open-access article distributed under the terms and conditions of the Creative Commons Attribution license (<http://creativecommons.org/licenses/by/4.0/>).